Optimized low-level liquid scintillation spectroscopy of ^{35}S for atmospheric and biogeochemical chemistry applications

Lauren A. Brothers, Gerardo Dominguez[1], Anna Abramian, Antoinette Corbin, Ben Bluen, and Mark H. Thiemens

Department of Chemistry and Biochemistry, University of California, San Diego, CA 92093-0356

Edited by Karl K. Turekian, Yale University, North Haven, CT, and approved January 12, 2010 (received for review February 02, 2009)

Anthropogenic activities, dominated by emissions of sulfur dioxide (SO_2), have perturbed the global sulfur (S) cycle. Uncertainties in timescales of S transport and chemistry in the atmosphere lead to uncertainties in the predicted impact of S emissions. Measurements of cosmogenic ^{35}S may potentially be used to resolve existing uncertainties in the photochemical and chemical transformation of S in the environment. The lack of a simple, effective, and highly sensitive technique to measure ^{35}S activity in samples with low activities may explain the scarcity of published measurements. We present a set of new sample handling and measurement procedures optimized for the measurement of ^{35}S in natural samples with activities as low as 0.20 dpm above background (2σ, integration time = 2 hr). We also report simultaneous measurements of aerosol ($^{35}SO_4$) and gas phase ($^{35}SO_2$) collected at inland and coastal locations; the range of observed activities corresponds to SO_2 residence lifetimes of 0.2 ± 0.04 (coastal) – 22.3 d± 0.04 (inland). These optimized techniques offer the potential for resolving atmospheric processes that occur on 6–12-hour timescales as well as resolving transport phenomena such as stratospheric mixing into the troposphere.

aerosol sulfate | sulfur cycle | dry deposition | sulfur dioxide residence times

According to the Intergovernmental Panel on Climate Change (1) anthropogenic emissions of sulfur dioxide have perturbed the sulfur cycle on local, regional, and global scales. These emissions and their oxidized end products lead to increases in acid rain (H_2SO_4) and aerosol sulfate (SO_4^{2-}) concentrations that play a significant role in climate and the global sulfur cycle. Sulfur-containing aerosol particles serve as cloud condensation nuclei affecting cloud formation and the hydrological cycle. Our knowledge of the chemical and photochemical processes that govern the chemical transformations and transport of sulfur compounds in the atmosphere is incomplete due to the complex, multivalent nature of sulfur and uncertainties in the understanding of aerosol chemistry. Sulfur in the atmosphere exists simultaneously as a solid and gas, further complicating matters. The development of new and/or improved analytical techniques to study the sulfur cycle on short timescales (hours to days) is, therefore, of considerable importance. Here we describe significant advances in the detection sensitivity of the cosmogenic isotope ^{35}S that can be used as a tracer of gas and aerosol phase lifetimes and turnover kinetics with high time and aerosol size resolutions.

Stable isotopic measurements of atmospheric species such as nitrate (NO_3^{1-}) and sulfate (SO_4^{2-}) have recently been used to provide strong constraints on the oxidative processing of their precursors, NO_x and SO_x, in the atmosphere (2–6). The radionuclide ^{35}S (β-decay to ^{35}Cl, $t_{1/2} = 87.4$ d) is continuously produced in the atmosphere by the interaction of cosmic rays with ^{40}Ar and provides an additional opportunity for tracing atmospheric processes. Upon production, ^{35}S rapidly oxidizes to ^{35}SO (lifetime < 1 ms) and to $^{35}SO_2$(~1 s) (7, 8). In the atmosphere, $^{35}SO_2$ undergoes wet deposition (removal below and within clouds), dry deposition (gravimetric settling or interactions with surfaces), or may be oxidized to sulfate ($^{35}SO_4^{2-}$) and incorporated onto aerosol particles (which eventually undergo dry and wet deposition). The sink reactions occur on timescales of a few hours to a few days, depending on the local atmospheric environment; thus the concentration of $^{35}SO_4^{2-}$ and $^{35}SO_2$ is expected to vary significantly as a function of time, meteorology, humidity, and location. These variables can vary on timescales of hours to days, which highlights the need of the present work of developing high time resolution measurement capabilities.

The chemical properties of $^{35}SO_2$ and $^{35}SO_4^{2-}$ are expected to be nearly identical to SO_2 and SO_4^{2-}, respectively. Measurements of ^{35}S in aerosol sulfate may be used to better resolve aerosol aging and chemistry, lifetimes of aerosol SO_4^{2-} and gas phase SO_2, and provide a better measure of boundary layer dynamics (9, 10). Previous ^{35}S measurements have been used to calculate SO_2 fluxes (9, 11–14) and depositional rates (wet and dry) (9, 12, 15, 16) and trace atmospheric sulfate deposition into lakes, rivers (17), and catchments (18–22). Some of these papers have included measurements of $^{35}SO_4^{2-}$ in *bulk* aerosols (9, 23).

Because the atmospheric aerosol chemistry of sulfur depends on the type, size, and number density of aerosol particles, one of the principal goals of this work is to improve existing measurement techniques so as to obtain particle-size-resolved measurements of ^{35}S in aerosol sulfate without the need to collect samples for long periods of time that may mask short-term variability.

Recently, a technique using low-level liquid scintillation spectroscopy (LSS) was developed to measure ^{35}S in lake water (17). Our review of this technique revealed that the methods used introduced high backgrounds, prohibiting their use for determining the activities of natural samples with low $^{35}S/S$ ratios. Here we present improved sample handling and analysis techniques employing LSS and our first field results. The improvements include unique sample preparation procedures, identification and correction of previously unreported backgrounds, as well as a method for optimizing the integration of scintillation spectra. Our improved methods allow for the measurement of the abundance of $^{35}SO_4^{2-}$ as a function of aerosol size as well as $^{35}SO_2$ with sample collection times as short as 12 hr at a coastal and an inland location at similar altitudes and latitudes. Using these measurements, we estimated the overall lifetime of SO_2 at these two locations.

Author contributions: L.A.B., G.D., and M.H.T. designed research; L.A.B., G.D., A.A., A.C., and B.B. performed research; L.A.B., G.D., A.A., A.C., and M.H.T. contributed new reagents/analytic tools; L.A.B., G.D., and M.H.T. analyzed data; and L.A.B., G.D., and M.H.T. wrote the paper.

The authors declare no conflict of interest.

This article is a PNAS Direct Submission.

[1]To whom correspondence should be addressed. E-mail: gdominguez@ucsd.edu

This article contains supporting information online at www.pnas.org/cgi/content/full/0901168107/DCSupplemental.

The increased sensitivity to ^{35}S concentrations presented in this paper should allow for the study of a broader range of environmental processes such as boundary layer dynamics, evolution of sulfate in aircraft plumes in the lower stratosphere, deposition of sulfate into the hydrological cycle, kinetics of SO_2 oxidation, and aerosol dynamics (including the transport and evolution of sulfur in remote locations such as Antarctica). In summary, the enhanced sensitivity of our method expands the range of biogeochemical processes that can now be explored.

Results and Discussion

Method Testing. A Wallac Quantalus 1220 Ultra Low-Level Liquid Scintillation Counter was used for all the measurements and optimization tests that we report here. This instrument minimizes cosmic ray backgrounds using passive and active shielding, multiple multichannel analyzers, and anticoincidence counting techniques. A $Na_2{}^{35}SO_4$ standard (MP Biomedical) was used to optimize the sample preparation techniques. The instrument's detection efficiency (ε_D) was determined using a calibrated (absolute) ^{14}C activity standard from Perkin Elmer (dpm $= 96,200$)* (24). By comparing the instrument reported count rate (counts per minute, cpm) and the expected activity (disintegrations per minute, dpm) for the absolute standard, the instrument's overall detection efficiency ($\varepsilon_D = \frac{\text{cpm}}{\text{dpm}}$) was determined to be 0.946. This efficiency is an upper limit to the overall efficiency of the detection technique presented here, since natural samples will also incur losses in their measured activity by being lost during preparation. Given the high activity of the ^{14}C standard, this efficiency determination is unaffected by electronic noise or sample vial backgrounds.

Energy channel optimization. The detection system bins photon pulse events into one of 1,024 energy channels, with the higher channels corresponding to highest energies. The β-decay spectrum of ^{35}S is well defined with a maximum decay energy of 0.1675 MeV (15). If the energy spectra of different cosmogenic species are sufficiently distinct, partial-to-complete discrimination between decay events of ^{35}S and those of other radionuclides present in the sample (e.g. ^{14}C) can be achieved by selective integration of the energy spectra. Fig. S1 displays the spectra measured for ^{35}S, ^{14}C, and radioactive isotopes of barium. While each channel contributes noise to the integrated count rate, integrating counts only in the energy range where ^{35}S decay events occur results in improved signal to noise ratios. In collected aerosol and gas samples, organic molecules containing ^{14}C may contribute to the background activity, and our optimization considers these contributions. Using the spectra shown in Fig. S1, the ratio of the time- and channel-integrated signal $[S_m(\text{ch1},\text{ch2})]$ and background $[B_m(\text{ch1},\text{ch2})]$ ratio can be used to optimize the counting of samples and is defined as

$$\frac{S_m(\text{ch1},\text{ch2})}{B_m(\text{ch1},\text{ch2})} = \frac{\sum_{i=\text{ch1}}^{\text{ch2}} \dot{S}_A(i)\cdot\Delta t}{\sum_{i=\text{ch1}}^{\text{ch2}} \dot{B}_A(i)\cdot\Delta t}, \qquad [1]$$

where ch1 and ch2 are the start and end channels of integration, respectively, and $\dot{S}_A(i)$ and $\dot{B}_A(i)$ are the observed count rates in channel i of ^{35}S and interfering backgrounds (including ^{14}C, radioactive barium isotopes, and/or scintillation gel). This ratio is plotted separately for the backgrounds expected from barium, the scintillation gel, and ^{14}C as a function of ch2 in Fig. S2. The ratio of $\frac{S_m}{B_m}$ reaches a maximum value close to the channel where the ^{35}S decay spectrum reaches its maximum (ch2 ~ 450). Integration between 1 (ch1) to 445 (ch2) and 455 (ch2) captures 95% and 97% of all decay events under the ^{35}S spectrum shown in Fig. S2 while minimizing background contributions.

Taking measurements of β^- activities using LSS requires using a scintillation gel that fluoresces when excited by emitted β^- particles as well as a vial to hold the sample-gel mixture. The choice of scintillation vial material, preparation techniques, and the amount of scintillation gel volume used can affect the sensitivity of measurements in LSS.

Major gains in sensitivity were attained by minimizing the background activities of scintillation vials and reagents used in the preparation of samples. The most significant background reductions were obtained by using plastic vials (Fisherbrand, 20 mL, ~0.145 dpm) as opposed to glass vials (Wheaton Glass-20 mL, 0.45 dpm). Similarly, glass fiber filters (Whatman GF/B), like those recommended by Hong and Kim (17) to isolate and count lake water sulfate as $BaSO_4$, also possessed relatively high activities (~2.6 dpm per 2×2 inch section). These activities likely originate from the decay ^{40}K present in borosilicate glass and, as a result, we avoided the use of glass vials and fiber paper in our subsequent tests and natural sample measurements. Microquartz filters were not tested in this study.

The scintillation gel contributes to the overall activity of a sample but is a strictly necessary reagent for measuring samples because of its role in converting the energy loss from a decay event into photons that are detected by the photomultiplier tubes of the Quantulus. The use of optimized integration channels (ch1 : ch2) resulted in a 30% reduction in the background contributed by the scintillation cocktail for a given gel volume (V_G). The activity measurements reported below use the optimized integration channels. Because measurements of empty vials yielded negligible (<0.01 dpm) activities, the observed background activity in scintillation vials filled with variable amounts of gel must come from the gel itself. This gel-specific background (B_G) is a nonlinear function of V_G and can be fit by a second-order polynomial with respect to V_G as

$$\dot{B}_G(V_G) = 0.188 + (0.1821)V_G - (0.002)V_G^2. \qquad [2]$$

Using a $Na^{35}SO_4$ (aq.) standard (MP Biomedical, ~4,000 dpm/mL of solution of H_2O) to ensure that $\frac{S_m}{B_m} \gg 1$, we determined the counting efficiency of the liquid scintillation technique for aqueous samples of volume 0.1 mL and 1 mL using various values of V_G. These counting efficiencies are shown in

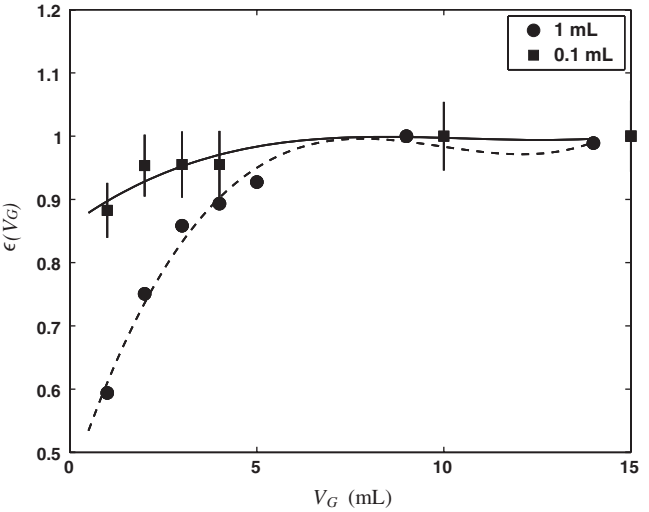

Fig. 1. ^{35}S decay event detection efficiency $[\varepsilon(V_G)]$ as a function of gel volume (V_G) used for 0.1 mL and 1 mL aqueous samples. Note that the counting efficiency exceeds 90% for smaller amounts of gel compared to aqueous samples with larger volumes.

*The lack of an absolute activity standard for ^{35}S and the significant overlap between the β^- spectra of ^{14}C and ^{35}S allows us to make this a reasonable substitution.

Fig. 1. Polynomial fits to these data yield the following counting efficiencies as a function of gel volume:

$$\varepsilon(V_G) = 0.4498 + (0.1782)V_G + (-0.0188)V_G^2 + (0.0006)V_G^3 \quad (1\text{ mL}), \qquad [3]$$

$$\varepsilon(V_G) = 0.8584 + (0.0428)V_G - (0.0042)V_G^2 + (0.0001)V_G^3 \quad (0.1\text{ mL}). \qquad [4]$$

Optimizing V_G to maximize sensitivity in weak samples. We determined the optimal scintillation gel volume as follows: We assumed that an aqueous sample of volume V_{SA} [0.1 or 1 mL of $NaSO_4$ (aq.)] is to be counted. Because we want to determine the sample's unknown activity $\dot{S}_A$ (dpm) in a gel volume V_G, we need to know what amount of gel volume maximizes our signal to noise. The expected signal, S_m, that is reported by the scintillation system during an integration time Δt is given by

$$S_m(V_G) = \varepsilon_{\text{prep}} \cdot \varepsilon_D \cdot \varepsilon_V(V_G) \cdot \dot{S}_A \Delta t, \qquad [5]$$

where ε_D is the overall detection efficiency of the Quantulus detection system (~0.94) and $\varepsilon_V(V_G)$ is the gel volume dependence of the detection efficiency (e.g. Eq. **3** or **4**) for an aqueous sample, and $\varepsilon_{\text{prep}}$ is the sample preparation efficiency. We note that in our tests with laboratory standards, the sample preparation efficiency was 100% ($\varepsilon_{\text{prep}} = 1$). The noise in the Quantalus scintillation spectroscopic system is dominated by fluctuations in the total number of events *detected* in the same time interval and is given by

$$\text{Noise}(V_G) = \sqrt{N_T} = \sqrt{S_m(V_G) + \dot{B}_G(V_G)\Delta t}. \qquad [6]$$

The ratio $\frac{S_m}{\sqrt{N_T}}$ is plotted as a function of V_G in Fig. 2 for a weak sample with $\dot{S}_A = 0.2$ dpm and $\Delta t = 1$ and 2 hr. Examination of Fig. 2 reveals that the signal to noise (and hence the minimum detection limit, MDL) can be maximized for 1 mL aqueous samples when $V_G = 2.5$ mL. Even more important, however, is the observation that smaller aqueous volumes, in this case 0.1 mL, yield substantially improved MDLs. The main reason for this behavior is that the efficiency of detection [$\varepsilon_V(V_G)$] as a function of V_G for 0.1 mL aqueous samples is already close to 90% when $V_G = 1$. Additional gains in efficiency obtained by using larger gel volumes are marginal and are offset by the higher backgrounds associated with the scintillation gel. Thus, contrary to previous method descriptions, we find that minimizing the gel volume can significantly improve the MDL for the LSS of ^{35}S.

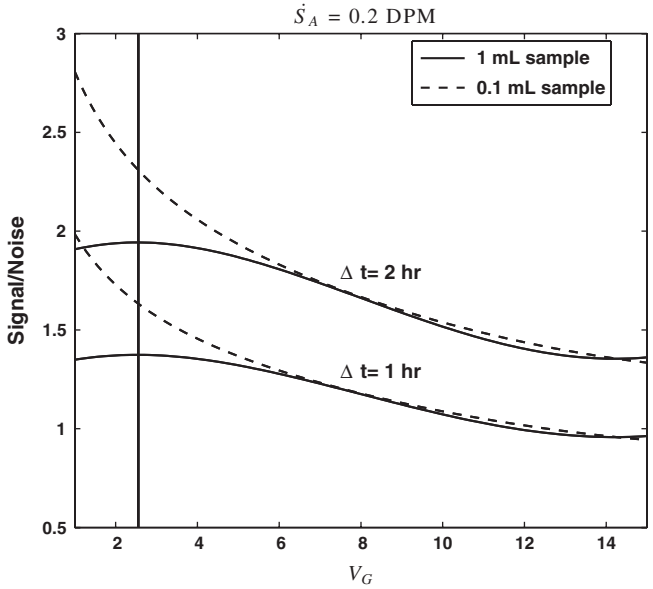

Fig. 2. Signal/noise ($\frac{S_m}{\sqrt{N_T}}$) for 0.1 and 1 mL aqueous samples as a function of gel volume. Note that smaller amounts of water lead to drastic improvements in the minimum detection limit.

Background interferences from barium isotopes. See *SI Methods*.

Preparation efficiency. See *SI Methods*.

Natural Sample Results. We collected and measured size-segregated (*SI Methods*) atmospheric aerosol and SO_2 samples at the Scripps Institute of Oceanography (SIO, latitude = 32.867°N, longitude = 117.257°W) and San Fernando Valley (SFV, latitude = 34.212°N, longitude = 118.061°W) during September 2007. These samples were processed before the optimized techniques described here were developed, and their activities were measured as $BaSO_4$. Size-segregated aerosol sulfate and gaseous SO_2 samples (*SI Methods*) were also collected during July 2008 and were measured as Na_2SO_4(aq). The uncertainties, determined by counting statistics, for the 2007 samples are larger than those associated with the 2008 samples due to the difficulties in preparing and measuring these samples as $BaSO_4$, as we have discussed in our measurement techniques. Overall, the background corrected activities we observed ranged from 0 (within the measurement uncertainty) to 22.20 ± 1.22 dpm (see Tables 1 and 2). All samples were recounted once the naturally present ^{35}S had fully decayed and were spiked with 0.1 mL of the ^{35}S standard. This procedure allowed us to correct for sample self-absorption of scintillation events. The corrected count rates are reported in Tables 1 and 2.

While detailed modeling of the observed absolute activities (dpm) is beyond the scope of this work, examination of the ^{35}S activity in the gas and aerosol phases points to the potential of the methods developed here to address present uncertainties in our understanding of the global S budget. We found, with the exception of a few days, that the activities contained within aerosol particles <1.5 μm were generally higher than those within particles of diameter >1.5 μm. Despite their proximate latitudes and longitudes, the activities in both size fractions were generally higher at SFV than at SIO. The fraction of non-sea-salt sulfate (NSS) was measured and calculated (*SI Methods*) for each sample using the total concentration of sulfate and sodium and the molar ratio of sulfate to sodium (0.0604) found in seawater. The SIO samples had a much higher fraction of the total sulfate derived from sea salt, with the coarse aerosols dominated by sea-salt sulfate. The lower ^{35}S activity in these samples is consistent with these aerosol particles being fresh sea-salt aerosols without any measurable amounts of secondary sulfate produced by the oxidation of $^{35}SO_2$. A few coarse samples at SIO have an activity >0, yet have Na^+ abundances that indicate that 100 ± 8% of the sulfate is from sea-salt spray. An estimate of the amount of non-sea-salt sulfate that would be needed to explain this apparent discrepancy was obtained using the molar ratio of $^{35}S/S$ ratio from SO_2 collected at SIO, and this estimate indicates that the activity falls within the total measurement uncertainty of the ion-chromatographic method used to determine the cation and anion concentrations.

To provide the proper context to relate our $^{35}SO_4$ and $^{35}SO_2$ concentration measurements (reported as activities) to atmospheric processes, we follow a treatment similar to that of Ref. 12 in relating the concentration of $^{35}SO_2$ to the overall lifetime of SO_2 (τ_{overall}) in an atmospheric box model. For a stable boundary layer and ignoring mixing from outside of this box, the time-dependent concentration of $^{35}SO_2$ can be expressed as

Table 1. ^{35}S activity of aerosol SO_4^{2-} found in particles >1.5 μm in size at Scripps Institution of Oceanography and San Fernando Valley

Sample	dpm per sample	$[^{35}SO_4]$ m^{-3}	dpm/μmol S	dpm/μmol nss-S	%NSS
SFV 9/3/2007*	4.90 ± 3.83	453 ± 347	0.21 ± 0.16	0.34 ± 0.26	60.2%
SFV 9/7/2007*	-2.06 ± 3.61	- 187 ± 328	-0.05 ± 0.09	-0.12 ± 0.21	42.9%
SFV 9/16/2007*	-0.88 ± 3.11	-80 ± 282	-0.02 ± 0.09	-0.05 ± 0.19	45.9%
SFV 7/21/2008	16.47 ± 1.06	1494 ± 96	0.43 ± 0.03	1.23 ± 0.08	34.9%
SFV 7/25/2008	-0.30 ± 1.33	-27 ± 121	-0.01 ± 0.03	-0.02 ± 0.11	29.4%
SFV 7/28/2008	5.62 ± 1.22	510 ± 111	0.16 ± 0.03	1.01 ± 0.22	15.5%
SVF 8/1/2008	3.84 ± 1.09	349 ± 99	0.09 ± 0.02	0.22 ± 0.06	39.8%
SIO 9/4/2007*	-0.021 ± 0.643	-2 ± 58	0 ± 0.01	-	0
SIO 9/7/2007*	-0.122 ± 0.653	-11 ± 59	0 ± 0.01	-	0
SIO 9/11/2007*	-0.138 ± 0.691	-16 ± 63	0 ± 0.007	-	0
SIO 7/21/2008	2.16 ± 0.84	196 ± 76	0.36 ± 0.14	-	0
SIO 7/25/2008	3.06 ± 0.86	278 ± 78	0.10 ± 0.03	-	0
SIO 7/28/2008	-1.62 ± 0.74	-147 ± 67	-0.06 ± 0.03	-	0
SIO 8/1/2008	2.26 ± 0.77	205 ± 70	0.07 ± 0.02	-	0

Samples measured as $BaSO_4$(s) are indicated using *. All other samples (2008) were measured as Na_2SO_4(aq). Air volume per sample (V_{air}) was equal to 2, 000 m^3 and the total number of ^{35}S(^{35}N) in each sample was determined using the relationship $^{35}N = \text{dpm} \cdot \frac{t_{1/2}^{min}}{\ln(2)}$, where $t_{1/2}^{min}$ is the radioactive-decay half-life of ^{35}S expressed in minutes and dpm is the measured activity of the sample in units of disintegrations per minute at the time of collection. The volumetric concentrations of ^{35}S were calculated as $[^{35}SO_4] = \frac{^{35}N}{V_{air}}$. Non-sea-salt sulfate was determined using anion and cation measurements of aerosol samples and the molar ratio of sulfate to sodium (0.0604) in sea-salt spray.

$$\frac{d[^{35}SO_2]}{dt} = P_{CR} - \frac{[^{35}SO_2]}{\tau_{ox}} - \frac{[^{35}SO_2]}{\tau_{dd}} - \frac{[^{35}SO_2]}{\tau_{wd}} - \frac{[^{35}SO_2]}{\tau_{decay}}, \quad [7]$$

where P_{CR} is the cosmic ray production rate of ^{35}S. The timescales for sinks of $^{35}SO_2$ are represented by an oxidative lifetime (τ_{ox}), a dry deposition lifetime (τ_{dd}), the lifetime with respect to wet deposition (τ_{wd}), and the radioactive lifetime (τ_{decay}) of ^{35}S (radioactive mean-life = 126 days). Combining all sink terms proportional to $[^{35}SO_2]$, defining $\frac{1}{\tau_{overall}} = \frac{1}{\tau_{ox}} + \frac{1}{\tau_{dd}} + \frac{1}{\tau_{wd}} + \frac{1}{\tau_{decay}}$, assuming steady-state conditions within the box ($\frac{d[SO_2]}{dt} = 0$), and solving the resulting expression for $\tau_{overall}$ yields

$$\tau_{overall} = \frac{[^{35}SO_2]}{P_{CR}}. \quad [8]$$

The production rate of ^{35}S in the troposphere reported by Ref. 13 of 4.75×10^{-4} atoms m^{-3} s^{-1} was used to determine the integrated production in a 10 km high volume. The results are presented in Table 3.

Inspection of Table 3 reveals significant and systematic differences in $\tau_{overall}$ between the inland (SFV) and oceanic (SIO) sites that likely reflect differences in the predominant mechanisms affecting the lifetime of SO_2 at these two locations. Given the absence of precipitation events during the sample collection times, we ignore the contribution of wet deposition ($\tau_{wd} \rightarrow \infty$). Surface resistance models indicate that large differences in deposition velocities (v_{dd}) exist for SO_2 over land (0.2–0.4 cm s^{-1}) and seawater (~0.8 cm s^{-1}) (25). For a mixing height of 1000 m, these v_{dd} values translate to deposition lifetimes of about 5.78–2.89 and 1.5 d for SFV and SIO, respectively. An additional factor that determines $\tau_{overall}$ at each of these locations is the removal of SO_2 by OH. This lifetime is given by

$$\tau_{ox} = \frac{1}{k_1 \langle [OH] \rangle_t}, \quad [9]$$

where k_1 is the effective rate constant for the reaction $SO_2 + OH \xrightarrow{k_1} HSO_3$ ($k_1 \sim 3 \times 10^{-12}$ cm^3 s^{-1}) (26), and $\langle [OH] \rangle_t$ is the time-averaged (over 24 hr) concentration of OH

Table 2. ^{35}S activity of aerosol SO_4^{2-} found in particles <1.5 μm in size at Scripps Institution of Oceanography and San Fernando Valley

Sample	dpm per sample	$[^{35}SO_4]$ m^{-3}	dpm/μmol S	dpm/μmol nss-S	%NSS
SFV 9/3/2007*	10.84 ± 2.87	984 ± 260	0.18 ± 0.05	0.28 ± 0.07	64.1%
SFV 9/7/2007*	13.63 ± 2.84	1236 ± 258	0.27 ± 0.06	0.40 ± 0.08	68.9%
SFV 9/16/2007*	13.18 ± 2.59	1196 ± 235	0.18 ± 0.03	0.27 ± 0.05	66.4%
SFV 7/21/2008	3.76 ± 1.06	341 ± 96	0.03 ± 0.01	0.03 ± 0.01	88.3%
SFV 7/25/2008	20.43 ± 1.33	1854 ± 121	0.10 ± 0.01	0.12 ± 0.01	88.7%
SFV 7/28/2008	22.20 ± 1.22	2013 ± 111	0.16 ± 0.01	0.19 ± 0.01	84.7%
SFV 8/1/2008	9.80 ± 1.09	889 ± 99	0.04 ± 0.00	0.04 ± 0.00	92.7%
SIO 9/4/2007*	-1.09 ± 2.53	-99 ± 230	- 0.01 ± 0.03	-0.01 ± 0.03	75.9%
SIO 9/7/2007*	-1.94 ± 2.29	-176 ± 207	-0.04 ± 0.05	-0.06 ± 0.07	67.3%
SIO 9/11/2007*	3.91 ± 2.45	355 ± 223	0.08 ± 0.05	0.13 ± 0.08	61.8%
SIO 7/21/2008	11.46 ± 0.97	1040 ± 88	0.55 ± 0.05	0.85 ± 0.07	64.0%
SIO 7/25/2008	3.26 ± 0.91	295 ± 83	0.03 ± 0.01	0.04 ± 0.01	81.4%
SIO 7/28/2008	0 ± 0.90	0 ± 82	0.00 ± 0.01	0.00 ± 0.02	72.2%
SIO 8/1/2008	6.39 ± 1.10	580 ± 99	0.06 ± 0.01	0.15 ± 0.03	37.0%

Samples measured as $BaSO_4$(s) are indicated using *. All other samples (2008) were measured as Na_2SO_4(aq). Air volume per sample (V_{air}) was equal to 2, 000 m^3 and the total number of ^{35}S(^{35}N) in each sample was determined using the relationship $^{35}N = \text{dpm} \cdot \frac{t_{1/2}^{min}}{\ln(2)}$, where $t_{1/2}^{min}$ is the radioactive-decay half-life of ^{35}S expressed in minutes and dpm is the measured activity of the sample in units of disintegrations per minute. The air volume concentrations of ^{35}S were calculated as $[^{35}SO_4] = \frac{^{35}N}{V_{air}}$. Non-sea-salt sulfate was determined using anion and cation measurements of aerosol samples and the ratio of sulfate to sodium (0.0604) in sea-salt spray.

Table 3. Summary of $^{35}SO_2$ concentrations and $\tau_{overall}$ estimated using Eq. [9] and $P_{CR} = 4.75 \times 10^{-4}$ atoms m^{-3} s^{-1}

Sample date	dpm per sample	$[^{35}SO_2]$ m^{-3}	$\tau_{overall}$ (days)
SFV			
7/21/2008	4.80 ± 0.19	436 ± 17	10.6 ± 0.4
7/25/2008	9.03 ± 0.18	820 ± 16	20.0 ± 0.4
7/28/2008	6.21 ± 0.17	565 ± 16	13.8 ± 0.4
8/1/2008	10.07 ± 0.19	915 ± 18	22.3 ± 0.4
SIO			
7/21/2008	0.10 ± 0.19	9 ± 17	0.2 ± 0.4
7/25/2008	1.19 ± 0.17	108 ± 15	2.6 ± 0.4
7/28/2008	2.02 ± 0.19	184 ± 17	4.5 ± 0.4
8/1/2008	1.81 ± 0.14	165 ± 12	4.0 ± 0.3

Air volume per sample (V_{air}) was equal to 2, 000 m^3 and the total number of $^{35}S(^{35}N)$ in each sample was determined using the relationship: $^{35}N = \text{dpm} \cdot \frac{t^{min}_{1/2}}{\ln(2)}$, where $t^{min}_{1/2}$ is the radioactive-decay half-life of ^{35}S expressed in minutes and dpm is the measured activity of the sample in units of disintegrations per minute. The air volume concentrations of ^{35}S were calculated as $[^{35}SO_2] = \frac{^{35}N}{V_{air}}$.

per cm^3. Inserting values typical of polluted environments ($\langle[OH]\rangle_t \sim 1 \times 10^6$ cm^{-3}) leads to estimates for $\tau_{ox} \sim 3$–4 d, although the oxidation lifetime of SO_2 in the free troposphere may be longer. At this time, we do not know why the SFV and SIO lifetimes are longer than expected based on oxidative and dry deposition considerations, but these differences may be due to boundary layer shifts and/or mixing of air from the free troposphere. Detailed modeling of these factors, in the future, should help in clarifying their importance.

A similar analysis can be made to interpret the $^{35}SO_4$ concentration data presented in Tables 1 and 2. To begin, we express the overall rate of change of $^{35}SO_4$ as

$$\frac{d[^{35}SO_4(\text{aerosol})]}{dt} = \frac{[^{35}SO_2]}{\tau_{ox}} - \frac{[^{35}SO_4]}{\tau_{dd}(SO_4)} - \frac{[^{35}SO_4]}{\tau_{wd}(SO_4)} - \frac{[^{35}SO_4]}{\tau_{decay}}, \quad [10]$$

where τ_{ox} is again the overall lifetime of SO_2, $\tau_{dd}(SO_4)$ and $\tau_{wd}(SO_4)$ are the dry and wet deposition timescales of aerosol sulfate, and τ_{decay} is defined as before. Given the ability to discriminate size-dependent activities in aerosols, the activity in aerosol sulfate can be subdivided into two size bins and expressed as

$$\frac{d[^{35}SO_4(F)]}{dt} = \frac{[^{35}SO_2]}{\tau_{ox}(F)} - \frac{[^{35}SO_4(F)]}{\tau_{dd}(SO_4(F))} - \frac{[^{35}SO_4(F)]}{\tau_{wd}(SO_4(F))} - \frac{[^{35}SO_4(F)]}{\tau_{decay}}, \quad [11]$$

and

$$\frac{d[^{35}SO_4(C)]}{dt} = \frac{[^{35}SO_2]}{\tau_{ox}(C)} - \frac{[^{35}SO_4(C)]}{\tau_{dd}(SO_4(C))} - \frac{[^{35}SO_4(C)]}{\tau_{wd}(SO_4(C))} - \frac{[^{35}SO_4(C)]}{\tau_{decay}}. \quad [12]$$

Here, the oxidative $[\tau_{ox}(F,C)]$, dry deposition $[\tau_{dd}(F,C)]$, and wet deposition $[\tau_{wd}(F,C)]$ lifetimes are broken up into two components to correspond to fine (F) and coarse (C) aerosols. Again, if we assume steady-state conditions and combine the sink terms into one overall timescale for fine and coarse aerosols ($\frac{1}{\tau_{overall}(SO_4(F,C))} = \frac{1}{\tau_{dd}(SO_4(F,C))} + \frac{1}{\tau_{wd}(SO_4(F,C))} + \frac{1}{\tau_{decay}}$), we find that

$$[^{35}SO_4(F)] = \left(\frac{\tau_{overall}(SO_4(F))}{\tau_{ox}(F)}\right)[^{35}SO_2], \quad [13]$$

and

$$[^{35}SO_4(C)] = \left(\frac{\tau_{overall}(SO_4(C))}{\tau_{ox}(C)}\right)[^{35}SO_2]. \quad [14]$$

The higher (lower) activities per unit volume observed in fine (coarse) aerosol particles, therefore, are expected to depend on (1) the concentration of $^{35}SO_2$, (2) the ratio of the overall residence time for fine (coarse) aerosol sulfate, and (3) the rate of SO_2 oxidation and incorporation into fine (coarse) aerosol particles. In this discussion, we neglect the possibility that ^{35}S found in fine aerosol particles may end up in coarse aerosol particles due to aerosol size growth dynamics, although these timescales (hours to days) are expected to depend on total particle concentrations and characteristic particle sizes (27), and this process may be important for very polluted environments such as SFV. If coagulation were the dominant mechanism affecting the relative ratio of activity in fine and coarse aerosols, however, we would expect to see the same ratio of ^{35}S to total S in both of these sizes. Given the above discussion, it is interesting to note that the days with nonzero activities in SIO coarse particles in 2008 also corresponded to days with the lowest (shortest $\tau_{overall}$) concentrations of $^{35}SO_2$. These observations are consistent with an increase of the heterogeneous processing of SO_2 onto coarse aerosol particles and not to changes in the deposition velocities of SO_2, which would only lead to a decrease in the $^{35}SO_2$ concentration. Given the prevalence of sea-salt particles as a medium for the aqueous phase oxidation of SO_2, we suggest that these observations may be consistent with enhanced uptake and aqueous phase oxidation of $^{35}SO_2$ during these time periods. Future work with larger datasets and detailed modeling of the coupled gas and aerosol phase chemistry and ambient meteorological conditions will be needed to fully interpret these types of results and their variation. We emphasize that without the optimized methods that we have developed, an in-depth examination of short timescale (~6–12 hours) processes would not be possible.

In contrast to SIO coarse particles (~0–3 dpm per 2000 m^3), the SFV coarse aerosol size fraction had significantly higher (~0–16 dpm per 2000 m^3) $^{35}SO_4$ concentrations. In light of Eqs. **13** and **14**, these differences may be explained in part by the higher concentrations of $^{35}SO_2$ seen at SFV (~4–10 dpm per 2000 m^3) compared to SIO (~0–2 dpm per 2000 m^3) and/or substantial differences in the aerosol age (lifetime).

We compare the ^{35}S measurements presented here to the pioneering work of Tanaka and Turekian (9), which reported ^{35}S activities in aerosols collected *weekly* in 1992 at New Haven, Connecticut. Air samples collected during July and August of 1992 were reported to have activities ranging from 1.1×10^{-3}–14.5×10^{-3} dpm/μmol S for SO_4 and 6×10^{-4}–2.2×10^{-3} dpm/μmol S for SO_2. We note that these values are significantly lower than our measurements, which are summarized in Table 1. These differences in the total-sulfur normalized values reported by Tanaka and Turekian (9) and the present values may result from the dilution generated by larger regional SO_2 fluxes emitted by coal burning in the eastern United States. These high sulfur coal emissions in essence dilute the ^{35}S activity when normalized to the total mass of S in aerosols. In contrast, California does not operate coal burning electric plants or have any other large sources of SO_2 that would dilute $^{35}SO_2$ by a comparable factor. These results highlight the utility of the ^{35}S, as first shown by Tanaka and Turekian (12), to understand differences in regional atmospheric chemistry and transport. Reporting ^{35}S activity with respect to sampled air volume minimizes the dilution effect described above, but normalization has other uses, and thus reporting in both units is advisable.

Conclusion

This work presents improved and optimized methods for measuring ^{35}S in natural samples. These methods have reduced the limit of detection down to 0.200 dpm or 36,000 ^{35}S atoms for a one-hour integration and have been shown to be suitable for measurements of $^{35}SO_4$ in size-segregated aerosols and $^{35}SO_2$. We have identified sensitivity-limiting backgrounds in chemical reagents used for sample preparation and these findings should be considered in future ^{35}S measurements. In light of this work, we suggest that reports of excess ^{35}S in aerosols, in comparison to ^{7}Be or ^{32}P, may be erroneously high due to the high backgrounds that may be introduced by barium and suggests that the conclusions of Osaki et al. (23) may need to be revised. We recommend that ^{35}S activity measurements should be made as $NaSO_4$ rather than $BaSO_4$ in weakly radiogenic samples.

In the present work we have also simultaneously measured $^{35}SO_2$ and aerosol $^{35}SO_4^{2-}$ in two distinct locations. The ^{35}S activity differences observed between the two locations, as well as the differences observed in the two aerosol size fractions, illustrates the ability of ^{35}S to further elucidate the local and regional cycling of SO_2 and aerosol SO_4. Given the observed ^{35}S concentrations and the minimum detection limits presented here, use of these techniques should allow for high time resolution studies of SO_2 and sulfate. While this work focused specifically on measurements of aerosol $^{35}SO_4^{2-}$ and $^{35}SO_2$, the techniques can be readily applied to measure ^{35}S in fog, rain, and snow. For example, given the production rates of ^{35}S (1.5 times that in troposphere) and the residence time of SO_4 in the stratosphere (~2.5 years) (28), we estimate that the concentration of $^{35}SO_4^{2-}$ in the stratosphere, $[^{35}SO_4(\text{strat})]$, is $\sim(50\text{–}300)[^{35}SO_4(\text{trop})]$, or $\sim 37,000\ ^{35}SO_4^{2}$ molecules per m^{-3}, based on the range of concentrations we report here. The enhanced sensitivities and techniques we present here could be used to measure $^{35}SO_4^{2-}$ in snow, and enhanced concentrations of $^{35}SO_4$ may be used as a proxy for stratospheric intrusions in Antarctica and in samples from other remote field locations.

Because of the length of biological cycles, this technique offers a unique way to measure ^{35}S in fast growing plants, phytoplankton, and bacteria and therefore could provide a unique radioactive tracer to understand these processes.

Methods

Low-level liquid scintillation spectroscopy, combined with a high activity $Na^{35}SO_4$ (aq.) standard, was used to develop the optimized ^{35}S sample preparation protocols. A multistage high-volume sampler was used for the aerosol and gas-phase S collections. Complete details can be found in *Results and Discussion* and in *SI Text*.

ACKNOWLEDGMENTS. We thank the anonymous reviewer and K. Turekian for their helpful and insightful comments that greatly improved this manuscript. We acknowledge Ivan Gaylor who donated the Quantulus and also D. Lal for insightful conversations. G.D. acknowledges the Camille and Henry Dreyfus Postdoctoral Program in Environmental Chemistry and the U.C. President's Postdoctoral Fellowship Program for their support. L.B. and A.A. acknowledge Eloise and Russ Duff and the Kents for their financial support.

1. Solomon S, et al. (2007) *IPCC, 2007: Climate Change 2007: The Physical Science Basis. Contribution of Working Group I to the Fourth Assessment Report of the Intergovernmental Panel on Climate Change* (Cambridge Univ Press, Cambridge, UK) p 996.
2. Thiemens MH (2006) History and Applications of Mass-Independent Isotope Effects. *Annu Rev Earth Pl Sc* 34(1):217–262.
3. Alexander B, et al. (2005) Sulfate formation in sea-salt aerosols: Constraints from oxygen isotopes. *J Geophys Res* 110:D10307.
4. Alexander B, Savarino J, Barkov NI, Delmas RJ, Thiemens MH (2002) Climate driven changes in the oxidation pathways of atmospheric sulfur. *Geophys Res Lett* 29(14):1685.
5. Alexander B, Savarino J, Kreutz KJ, Thiemens MH (2004) Impact of preindustrial biomass-burning emissions on the oxidation pathways of tropospheric sulfur and nitrogen. *J Geophys Res* 109:D08303 doi: 10.1029/2003JD004218.
6. Lee CCW, Thiemens MH (2001) The $\delta^{17}O$ and $\delta^{18}O$ measurements of atmospheric sulfate from a coastal and high alpine region: A mass-independent isotopic anomaly. *J Geophys Res-Atmos* 106(D15):17359–17373.
7. Black G, Sharpless RL, Slanger TG (1982) Rate coefficients at 298 K for SO reactions with O_2, O_3, and NO_2. *Chem Phys Lett* 90(1):55–58.
8. Robertshaw JS, Smith IWM (1980) Rate data for $O + OCS \rightarrow SO + CO$ and $SO + O_3 \rightarrow SO_2 + O_2$ by a new time-resolved technique. *Int J Chem Kinet* 12(10):729–739.
9. Tanaka N, Turekian KK (1995) Determination of the dry deposition flux of SO_2 using cosmogenic ^{35}S and ^{7}Be measurements. *J Geophys Res-Atmos* 100(D2):2841–2848.
10. Turekian KK, Graustein WC (2003) Natural radionuclides in the atmosphere. *Treatise on Geochemistry*The Atomosphere, eds HD Holland and KK Turekian (Elsevier-Pergamon, Oxford), (ed RF Keeling), Vol 4, pp 261–279.
11. Junkermann W, Roedel W (1983) Evidence for short SO_2 lifetimes in the atmosphere: An in-situ measurement of atmospheric SO_2 lifetime using cosmic ray produced Sulphur-38. *Atmos Environ* 17(12):2549–2554.
12. Tanaka N, Turekian KK (1991) Use of cosmogenic ^{35}S to determine the rates of removal of atmospheric SO_2. *Nature* 352(6332):226–228.
13. Turekian KK, Tanaka N (1992) The use of atmospheric cosmogenic ^{35}S and ^{7}Be in determining depositional fluxes of SO_2. *Geophys Res Lett* 19(17):1767–1770.
14. Calvert JG, Chatfield RB, Delany AC, Martel EA (1985) Evidence for short SO_2 lifetimes in the atmosphere: An in-situ measurement of atmospheric SO_2 lifetime using cosmic ray produced ^{38}S. *Atmos Environ* 19(7):1205–1206.
15. Goel PS, Jha S, Lal D, Radhakrishna P, Rama P (1956) Cosmic ray produced beryllium isotopes in rain water. *Nucl Phys* 1(3):196–201.
16. Lal D, Arnold JR, Honda M (1960) Cosmic-ray production rates of ^{7}Be in oxygen, and P^{32}, P^{33}, S^{35} in argon at mountain altitudes. *Phys Rev* 118(6):1626–1632.
17. Hong YL, Kim G (2005) Measurement of cosmogenic ^{35}S activity in rainwater and lake water. *Anal Chem* 77(10):3390–3393.
18. Kester C, Baron J, Turk J (2003) Isotopic study of sulfate sources and residence times in a subalpine watershed. *Environ Geol* 43(5):606–613.
19. Novák M, Michel RL, Přechová E, Štěpánová M (2004) The missing flux in a ^{35}S budget for the soils of a small polluted catchment. *Water Air Soil Poll* 4(2–3):517–529.
20. Sueker JK, Turk JT, Michel RL (1999) Use of cosmogenic ^{35}S for comparing ages of water from three alpine-subalpine basins in the Colorado Front Range. *Geomorphology* 27(1-2):61–74.
21. Cape J (1993) The use of ^{35}S to study sulphur cycling in forests. *Environ Geochem Hlth* 15(2–3):113–118.
22. Michel RL, Turk JT, Campbell DH, Mast MA (2002) Use of natural ^{35}S to trace sulphate cycling in small lakes, Flattops Wilderness Area, Colorado, USA. *Water Air Soil Poll* 2(2):5–18.
23. Osaki S, Tagawa Y, Chijiiwa T, Sugihara S, Maeda Y (1999) Atmospheric deposition of ^{35}S. *J Radioanal Nucl Ch* 239(3):543–547.
24. Buckley JP (1970) The use of carbon-14 as a secondary counting standard for sulphur-35. *Int J Appl Radiat Is* 22:41–42.
25. Yiwen Y, Carmichael G (1998) Modeling the dry deposition velocity of sulfur dioxide and sulfate in Asia. *J Appl Meteorol* 37:1084–1099.
26. Sander SP, et al. (2006) *Chemical Kinetics and Photochemical Data for Use in Atmospheric Studies: Evaluation Number 15* (Jet Propulsion Laboratory, Pasadena), JPL Publication 06-2.
27. Seinfeld JH, Pandis SN (2006) *Atmospheric Chemistry and Physics* (Wiley-Interscience, New York).
28. van Velthoven PFJ, Kelder H (1996) Estimates of stratosphere-troposphere exchange: Sensitivity to model formulation and horizontal resolution. *J Geophys Res* 101:1429–1434.